INTERNATIONAL JOURNAL OF CHEMICAL REACTOR ENGINEERING

Volume 6 2008 *Article* A41

Studies on the Fluidized Bed Electrode

Siva Kumar* Thilakavathi Ramamurthy†
Bala Subramanian‡ Ahmed Basha**

*Anna University-Chennai, sivakumar.k@ge.com
†Anna University-Chennai, tika2k3@yahoo.co.in
‡Anna University-Chennai, nbsbala@annauniv.edu
**Central Electrochemical Research Institute, cab_50@yahoo.co.in

ISSN 1542-6580

Studies on the Fluidized Bed Electrode*

Siva Kumar, Thilakavathi Ramamurthy, Bala Subramanian, and Ahmed Basha

Abstract

The present investigation attempts to study the hydrodynamic characteristics of the fluidized bed electrode. A core-annular flow model with a transfer of particles between core-annular layers has been proposed to describe the flow behavior of conducting particles in the fluidized bed electrode. The effect of individual parameters on the rate of the particle transfer across the layer and thickness of the core-annular has been critically examined and the model simulation has been verified with the data reported in the literature.

KEYWORDS: fluidized bed electrode, modeling, potential distribution

*Corresponding author: Bala Subramanian; e-mail: nbsbala@annauniv.edu; Phone: 91-44-2220 3501; Fax: 91-44-2235 5373.

1. INTRODUCTION

The quantum of wastewater generated is increased proportionately with industrial revolution and day-to-day human activities. Industries such as textile, refineries, chemical, plastic and food-processing plants share major portion of wastewaters generated in chemical process industries. The effluents from these industries are characterized by a perceptible content of organics (e.g. phenolic compounds) with strong in colour. The global pollution including the contamination, over-use and mismanagement of water resources becomes a major threat. In consequence, the major issue in technological development focuses on protection of the environment and the preservation of resources; in particularly for wastewater discharge to the aquatic environment, waste emission limits are determined to prevent pollution.

Conventionally industrial effluents containing organics are treated with adsorption, biological oxidation, coagulation, etc. Though the conventional methods have some advantages, they are lacking of effectiveness if applied individually. Due to the large variability of the composition of wastewater, most of the traditional methods are becoming inadequate. As environmental regulations become stringent, new and novel processes for efficient treatment of various kinds of wastewater at relatively low operating cost are needed. In this context, researchers are trying various alternative processes such as electrochemical technique, wet oxidation, ozonization, and photo catalytic method for the degradation of organic compounds. Among these advanced processes, the electrochemical technique has been receiving greater attention in recent years due to its unique features such as versatility, energy efficiency, automation and cost effectiveness (Guohua Chen, 2004).

Due to large capital investment and the expensive recurring cost, electrochemical water or wastewater technologies did not find wide application worldwide then. With extensive research and development throughout the world, abundant knowledge has been gained resulting in very low cost effective electrochemical treatment techniques for various applications. The electrochemical technologies have reached a stage that they are not only comparable with other technologies in terms of cost but also are more efficient and compact.

In electrochemical technique, the main reagent is the electron, which is called ‘Clean Reagent’, and degrades all the organics present in the effluent without generating any secondary pollutant or bi-product/sludge. The electrochemical technique offers high removal efficiencies and lower temperature requirements compared to non-electrochemical treatments. In addition to the operating parameters, the rate of pollutant degradation depends on the anode material. When electrochemical reactors operate at high cell potential, the anodic

process occurs in the potential region of water discharge, hydroxyl radicals are generated. On the other hand, if chloride is present in the electrolyte, an indirect oxidation via active chlorine can be operative (Kazdobin et al., 2000). Several types of electrochemical reactors are used in process industries for various purposes. Fluidized-bed electrodes (FBE) is one such type finds extensive applications in chemical process industries as it offer large transfer area between the phases, improved heat and mass transfer between the phases and suitability for large scale operation (Fleischmann et al., 1971).

1.1 Fluidized Bed Electrode

Fluidization is a technique whereby fine solids are contacted with fluid to transform into a fluid-like state for purposes of mass/or heat transfer between the phases with or without simultaneous chemical reaction. The fluid may be a gas or liquid and depending on the flow rates and the properties of the contacting phases, the characteristics of the fluidized bed vary considerably.

Fluidized bed finds applications in chemical process industries as they provide large interfacial area, high degree of mixing, and temperature uniformity. Liquid-solid fluidized beds are increasingly used in chemical processes such as fermentation, biological wastewater treatment, flue gas desulphurization, ore reduction etc. Liquid solid fluidized beds are generally operated in a batch regime with respect to solid phase and as a continuous reactor with respect to liquid phase. In recent years, the fluidized bed applications are extended for electrochemical processes such as electro oxidation, cathodic reduction and metal recovery from dilute solution. The understanding of the flow regimes in fluidized bed reactors is the key for successful design and scale-up of these reactors.

Extensive work has been reported on fluidized bed electrode in environmental applications. Backhurst et. al., (1969) demonstrated the cathodic reduction of m-nitro benzene sulfonic acid to metaanilic acid in aqueous sulphuric acid and reported that the performance of fluidized bed electrode is very much dependent on the degree of fluidization. Welmers et al., (1977) reported the charge transfer mechanism in fluidized bed electrode. LeRoy (1978a, 1978b) studied electrowinning of copper from dilute solution using fluidized bed electrode operated at different regimes and proposed a model for electro winning of copper particles. Couret (1980) critically reviewed the application of fluidized bed electrode for recovery of metal from dilute solutions. Fluidized bed electrochemical reactor has been demonstrated for organic pollutant degradation by Zhou and Wu (2004). The authors oxidized p-nitrophenol using fluidized bed electrode and reported more than 90% efficiency. The electrochemical characteristics of graphite coated tin oxide particles have been studied by Lee and Ryu (2002) for chemical vapour deposition.

A critical review of the literature shows that though there has been good amount of work reported on fluidized bed electrode, the reported literature has its own limitations. Further no systematic model has been developed based on fundamental concept to describe the flow characteristic of conducting particles inside the reactor. In fluidized bed electrode, the conducting particles play an important role in maintaining bed voidage and current distribution and hence a systematic study of hydrodynamic behavior of conducting particles in fluidized bed becomes significant. The objective of the present work is to study the hydrodynamic behavior of the conducting particles in the riser of fluidized bed. A core-annular flow model with transfer of particles between core-annular layers has been proposed to demonstrate the flow behavior of conducting particles in the fluidized bed electrode. The effects of individual parameters on the rate of particle transfer across the layers and thickness of core-annular have been critically examined. The bed voidage estimated using the proposed model is incorporated in potential and current distribution estimation.

2. MODEL DEVELOPMENT

In fluidized bed electrode, when the electrolyte velocity exceeds the minimum fluidization velocity, the particles expands smoothly and rise to the upper layer and falls down, enhance mixing of dispersed phase. Further increase in the electrolyte velocity, the bed expands vigorously results improved solids mixing. Several models have been proposed to describe the flow behavior of solids particles in the fluidized bed. In the present study, a core annular model is proposed to describe the flow behavior of the conducting particles in the bed (Figure 1).

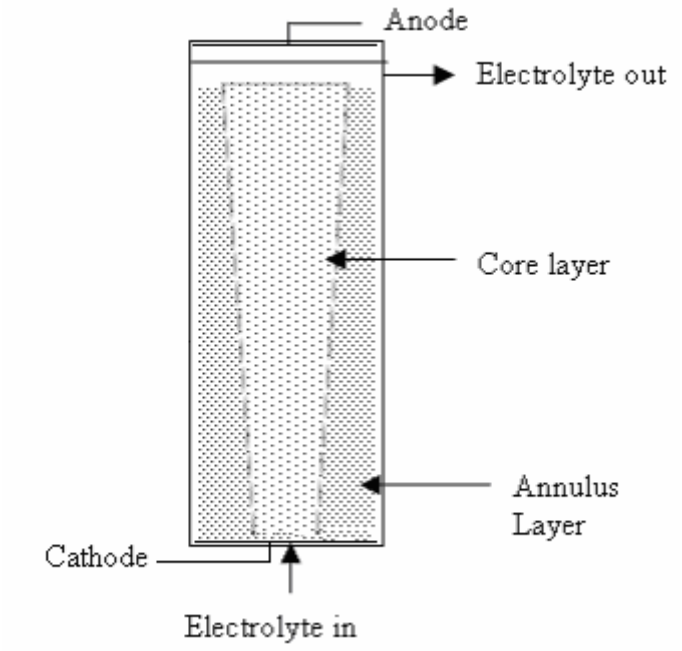

Figure 1: Schematic diagram Core-Annular flow structure.

The following assumptions are considered in developing the model equations (Rhodes 1990; Yerushalmi et al., 1978; Helland et al., 2000; Afsin and Nurdil, 2007).

In core region, solids flow

i. The flow structure consists of core–annular region, i.e. the reactor consists of dilute core region at the centre of the reactor surrounded by dense annular region in radial direction.
ii. The conducting particles flow up in dilute phase in the core region at the centre of the bed and move as dense phase in the annular region.
iii. Most of the electrolyte flow through the dilute region
iv. The particles move as single particles. The particle-particle hindrance effect is assumed to be negligible.
v. There is a net transfer of solids particles between core and annular region.
vi. The superficial velocity is much higher than the terminal velocity of the single particle.

Based on the above assumptions, the balance equations for the core layer and annular layer have been developed. The pressure balance equation for the core layer can be written as

$$\Delta P_c = g(\rho_S - \rho_l)(1-\varepsilon_c)L_c \quad (1)$$

where ΔP_c represents the total pressure drop in the core region and $g(\rho_S - \rho_l)$ represents the specific weight of the solid suspension. Similarly the pressure balance can be written for the annular layer as

$$\Delta P_a = g(\rho_S - \rho_l)(1-\varepsilon_a)L_a \quad (2)$$

The bed expansion in liquid-solid fluidized bed plays an important role as it directly influences the contact between the phases. The bed expansion of liquid-solid fluidized bed can be written as (Miura et al., 2001)

$$\frac{U_{slip}}{U_t} = \varepsilon^n \quad (3)$$

where, U_{slip} and U_t represent the slip velocity and particle terminal velocity respectively. The exponent `*n*' in equation (3) is function of particle Reynolds number, i.e.,

$$\begin{aligned} n &= 4.65 && \mathrm{Re}_t < 0.2 \\ n &= 4.45\,\mathrm{Re}_t^{-0.03} && 0.2 < \mathrm{Re}_t < 1 \\ n &= 4.45\,\mathrm{Re}_t^{-0.1} && 1 < \mathrm{Re}_t < 500 \\ n &= 2.39 && 500 < \mathrm{Re}_t \end{aligned} \quad (4)$$

The particle terminal velocity can be written as (Kunii and Levenspiel, 1969)

$$U_t = \frac{g(\rho_S - \rho_l)d_p^{\,2}}{18\mu_l} \qquad \mathrm{Re}_s < 0.4 \quad (5)$$

$$U_t = \left[\frac{4}{225}\frac{(\rho_S - \rho_l)^2 g^2}{\rho_l \mu_l}\right]^{1/3} d_p \qquad 0.4 < \mathrm{Re}_s < 500 \quad (6)$$

$$U_t = \left[\frac{3.1(\rho_S - \rho_l)g d_p}{\rho_l}\right]^{1/2} \qquad 500 < \mathrm{Re}_s \quad (7)$$

The bed voidage in liquid-solid fluidized bed can be considered to depend on slip velocity and particle characteristics, i.e.

$$\varepsilon = f\left(U_{slip}, d_p, \rho_s\right) \quad (8)$$

Slip velocity is defined as the relative velocity difference between the phases, which can be written as,

$$U_{slip} = \frac{U_l}{\varepsilon} \pm \frac{U_s}{1-\varepsilon} \tag{9}$$

where U_l and U_s represent the liquid and solids superficial velocity respectively. The positive/negative sign represents a generalized slip condition, which can be extended to represent the system with specific notation. For the present case, the equation (9) can be written as,

$$U_{slip_c} = \frac{U_l}{\varepsilon} - \frac{U_s}{1-\varepsilon} \tag{10}$$

where, U_{slip_c} represent the slip velocity in the core layer. Comparing equations (3) and (10) and incorporating the terminal and slip velocity for the core layer yields the following equation, i.e.,

$$U_{slip_C} = \left(\frac{3.1 g d_p (\rho_S - \rho_l)}{\rho_l} \right)^{\frac{1}{2}} {\varepsilon_C}^n \tag{11}$$

The annular layer is considered as expanded packed bed with upward electrolyte flow and downward solid flow. The pressure drop in the annular layer can be estimated using Ergun equation (Savinell and Dweik, 1996),

$$-\left(\frac{dp}{dz}\right) = \left(\frac{150(1-\varepsilon_a)^2 \mu_l U_{slip_a}}{{d_p}^2 {\varepsilon_a}^3} \right) + \left(\frac{1.75(1-\varepsilon_a)\rho_l {U_{slip_a}}^2}{d_p {\varepsilon_a}^3} \right) \tag{12}$$

The equation (12) can be integrated for the entire bed in order to get the total pressure drop in the annular layer and combined with equation (2) to get the slip velocity in the annular layer, i.e.,

$$U_{slip_a} = -\left(\frac{4286 \mu_l (1-\varepsilon_a)}{d_p \rho_l} \right) + \sqrt{\left(\frac{4286 \mu_l (1-\varepsilon_a)}{d_p \rho_l} \right)^2 - \left(\frac{g d_p {\varepsilon_a}^3 (\rho_S - \rho_l)}{1.75(1-\varepsilon_a)\rho_l} \right)} \tag{13}$$

where, $U_{slip_a} = U_{la} - U_{Sa}$ represent the slip velocity in the annular layer. The individual phase velocities are calculated from the slip velocity. As stated earlier, the solid particles move from core to annular resulting in exchange of conducting particles between core and annular regions. The solid particle velocity in the core

layer can be written as (Rhodes, 1990)

$$\Delta U_{sc} = \frac{-4K(1-\varepsilon_c)\Delta L}{D\alpha^2} \tag{14}$$

It is assumed that no particles leave the bed, resulting that the solids flow rate in the annular layer is equal to solid flow rate in the core layer, i.e.

$$M_{Sa} = -M_{Sc} \tag{15}$$

The negative sign indicates that the flow is in opposite direction. Expansion of equation (15) results

$$U_{Sa}(1-\varepsilon_a)\rho_S(1-\alpha^2)A = -U_{Sc}(1-\varepsilon_c)\rho_S\alpha^2 A \tag{16}$$

The equation (16) can be rearranged as,

$$U_{Sa} = -\left(\frac{U_{Sc}(1-\varepsilon_c)\alpha^2}{(1-\varepsilon_a)(1-\alpha^2)}\right) \tag{17}$$

where U_{sa} represents the particle velocity in the annular layer, ε_a, ε_c represent the bed voidage in core and annular layer respectively. While α represent the core layer thickness. Similarly for continuous phase, the inlet flow rate to the bed can be related as

$$Q = U_{La}\,\varepsilon_a(1-\alpha^2)A + U_{Lc}\varepsilon_c\alpha^2 A \tag{18}$$

The first term in the right hand side of equation represents the continuous phase flow rate in the annular layer while the second term represents the continuous phase flow rate in the core layer. The particle balance equation for the bed can be written as

$$(1-\varepsilon_a)(1-\alpha^2)L_a + (1-\varepsilon_c)\alpha^2 L_c = (1-\varepsilon_O)L_O \tag{19}$$

where L_c and L_a represent the bed height in the core and annular region respectively. The annular layer voidage can be calculated from the value of α and ε in the core layer. The pressure balance equation for the core and annular layers can be equated for the equilibrium conditions as follows

$$g(\rho_S - \rho_l)(1-\varepsilon_c)L_c = g(\rho_S - \rho_c)(1-\varepsilon_a)L_a \quad (20)$$

where $g(\rho_S - \rho_l)$ represent the solids suspension density. Solving the above equation, the voidage in the core layer and annular layers can be related as

$$\varepsilon_c = 1-(1-\varepsilon_a)L_a/L_c \quad (21)$$

The model predicts the bed voidage for the given operating conditions. The parameters used in the present model simulations are given in Table 1 and the algorithm for solving the above equations (1) to (21) is given in Table 2. The control of reactions in an electrochemical cell may be achieved by cell current or electrode potential regulation. The predicted bed voidage and velocity based on the present model have been used to estimate the current and potential distribution in the fluidized bed electrode. To illustrate, let us consider a simple electrode reaction

$$A + Ne^- \rightarrow B^+ \quad (22)$$

Table 1: The parameters used in the model simulation.

Independent variable	Symbol	Values used
electrolyte viscosity	μ_l	0.001 Kg m^{-1} s^{-1}
Electrolyte density	ρ_l	1000 Kg m^{-3}
Core layer height / Annular layer height	L_c / L_a	1.2
Initial height of the bed	Lo	$20x10^{-2}$ m
Solid particle	d_p: 500-800μm	ρ_s: 8900 kg $m^{-3}$and ρ_s: 11340 kg m^{-3}
Diffusivity	D_s	$0.67x10^{-9}$ m^2 s^{-1}
Pure electrolyte conductivity	κ_{lo}	8 S m^{-1}
Pure electrode conductivity	κ_{So}	600 S m^{-1}
Initial concentration	C_i	0.0005 M
Final Concentration	C_{out}	0.00005 M
Pore diameter	d	20 μm
Number of electrons involved	N	2

In general, the electrochemical reactions are controlled either by diffusion or kinetic. A typical fluidized bed electro-winning process has been considered to verify the simulation of proposed hydrodynamic model to electrochemical process. The system is assumed to follow one dimensional flow and operating under limiting current density. Accordingly, the balance equations can be developed (Scott, 1991). The convective diffusion equations can be written as

$$D_a \frac{\partial^2 C_i}{\partial x^2} + D_r \frac{\partial^2 C_i}{\partial y^2} - U_{lc} \frac{\partial C_i}{\partial x} - R(C_i, \eta) = 0 \qquad (23)$$

where, D_a and D_r represent the diffusivity and dispersion coefficient in x and y co-ordinate.

Table 2: Algorithm for solving the mathematical model.

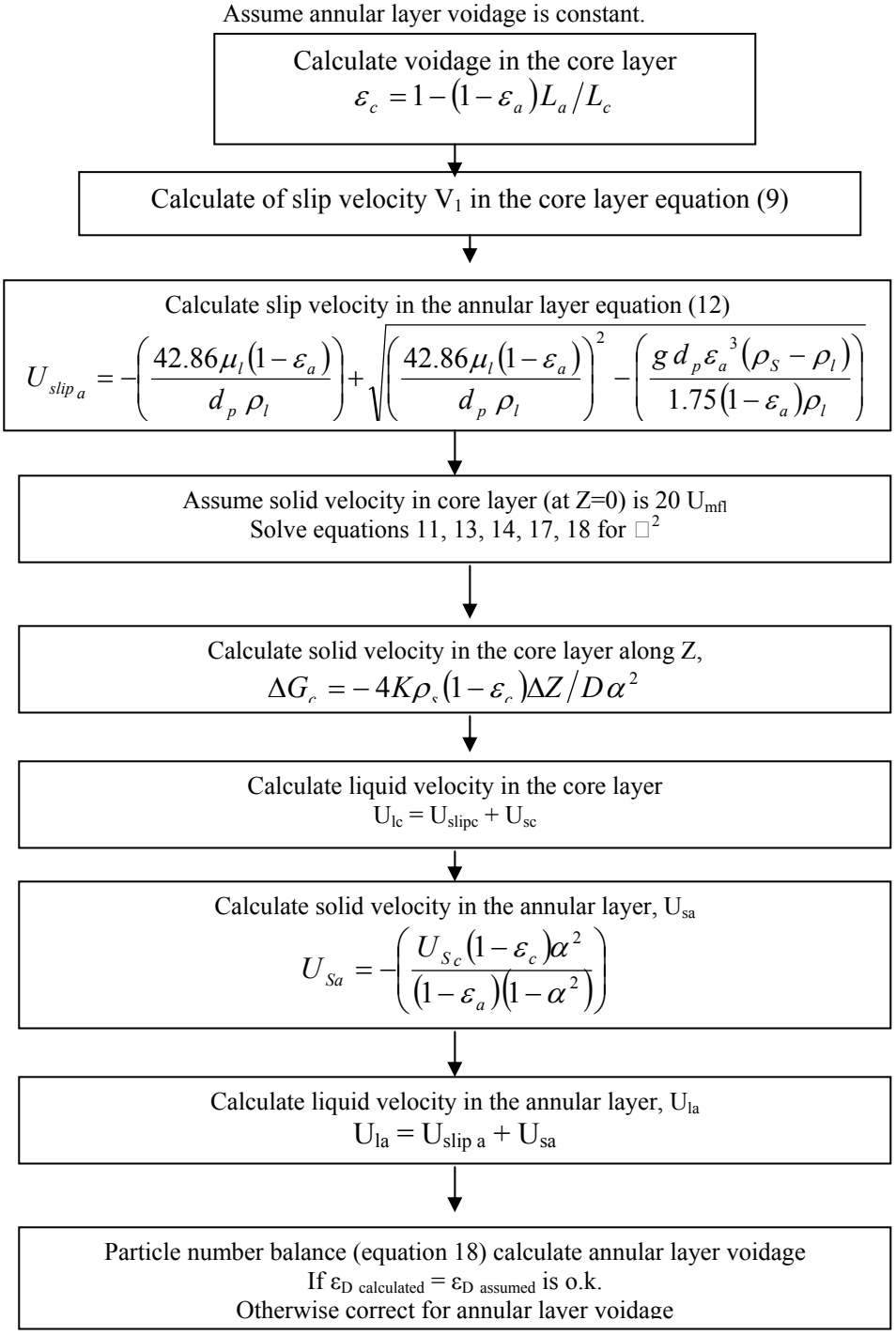

The electrode charge can be written as

$$\kappa_s\left(\frac{\partial^2\phi_s}{\partial x^2}+\frac{\partial^2\phi_s}{\partial y^2}\right)-NFR(C_i,\eta)=0 \tag{24}$$

Similarly the balance for the electrolyte phase can be written as

$$\kappa_l\left(\frac{\partial^2\phi_0}{\partial x^2}+\frac{\partial^2\phi_0}{\partial y^2}\right)+NFR(C_i,\eta)=0 \tag{25}$$

where k_l and k_s are the conductivities of electrolyte and conducting particle respectively.

The feeder and counter electrodes are arranged such that the current flow can be assumed to one dimensional. Further the diffusion and the dispersion effects are ignored. The equations (23) to (25) can be simplified to

$$U_{lc}\frac{dC_i}{dx}+R(C_i,\eta)=0 \tag{26}$$

$$\kappa_s\frac{\partial^2\phi_s}{\partial x^2}-NFR(C_i,\eta)=0 \tag{27}$$

$$\kappa_l\frac{\partial^2\phi_0}{\partial x^2}+NFR(C_i,\eta)=0 \tag{28}$$

The equation (26) to (28) can be written in terms of conversion as

$$U_{lc}C_i\frac{dX_i}{dx}+R'(X_i,\eta)=0 \tag{29}$$

$$\kappa_l\frac{\partial^2\eta}{\partial x^2}+NFR(C_i,\eta)=0 \tag{30}$$

With the assumption of limiting current operation, the electrolyte current density, i_s in the bed is proportional to the local concentration and related to the electrolyte potential gradient as

$$i_l=-\kappa_l\frac{d\phi_0}{dx} \tag{31}$$

Combining equations (29) and (31) results

$$\frac{di_l}{dx}=-U_{lc}NFC_i\frac{dX_i}{dx} \tag{32}$$

The current density along the reactor can be obtained by integrating the above equation as

$$i_l = U_{lc} NFC_i \left(\exp\left(\frac{-aK_m L}{U_{lc}} \right) + 1 - X_i \right) \tag{33}$$

Combining the equation (33) with the equation (31) and integrating for the reactor length results the variation of electrolyte potential, i.e.

$$\Delta\phi_0 = \frac{U_{lc} NFC_i}{aK_m \kappa_l} \left(\frac{aK_m L(1 - X_i)}{U_{lc}} - X_i \right) \tag{34}$$

Since the system is fluidized bed system, the conductivity of electrolyte phase is related to their pure conductivities as

$$\kappa_l = \kappa_{l0} \frac{2\varepsilon_c}{3 - \varepsilon_c} \tag{35}$$

The mass transport coefficient K_m can be estimated using the following equation (Good ridge and Scott, 1995)

$$K_m = 0.71 U_{lc} \left[\frac{U_{lc} d_p \rho_l}{\mu_l (1 - \varepsilon_c)} \right]^{-0.33} \left[\frac{\mu_l}{\rho_l D_S} \right]^{-0.67} \tag{36}$$

The equations (22) to (36) give the theoretical analysis of potential and current distribution in the fluidized bed electrode. The equations can be solved to obtain the current and potential distributions. The algorithm developed for solving the above equations (22) to (36) is given in Table 3.

3. MODEL SIMULATION AND DISCUSSION

For the model simulation, the diameter and height of the fluidized bed electrode have been assumed to be 43mm and 20cm respectively. The electrolyte is fed at the bottom of the column and discharged at the top of the bed. The effects of parameter such as particle diameter, particle density, solution properties and flow rate on the hydrodynamic behavior of the system have been critically examined. The model simulations under various operating conditions are presented in Figures 2 to 14.

Table 3: Algorithm for solving current and potential distribution.

Assume one dimensional flow

Balance equation electrolyte phase

$$U_{lc}\frac{dC_i}{dx}+R(C_i,\eta)=0$$

$$\kappa_l\frac{\partial^2\phi_0}{\partial x^2}+NFR(C_i,\eta)=0$$

Assume metal phase are equipotential the above equations and can be written in terms of conversion X_i as,

$$U_{lc}C_i\frac{dX_i}{dx}+R'(X_i,\eta)=0$$

$$\kappa_l\frac{\partial^2\eta}{\partial x^2}+NFR(C_i,\eta)=0$$

Assumption limiting current operation, the electrolyte current density i_l is given as

$$i_l=U_{lc}NFC_i\left(\exp\left(\frac{-aK_mL}{U_{lc}}\right)+1-X_i\right)$$

The current density in the solution, i_s, is related to the electrolyte potential gradient by the equation,

$$i_l=-\kappa_l\frac{d\phi_0}{dx}$$

Combining the above equations and integrating with x=L gives the variation in electrolyte potential, which is given as,

$$\Delta\phi_0=\frac{U_{lc}NFC_i}{aK_m\kappa_l}\left(\frac{aK_mL(1-X_i)}{U_{lc}}-X_i\right)$$

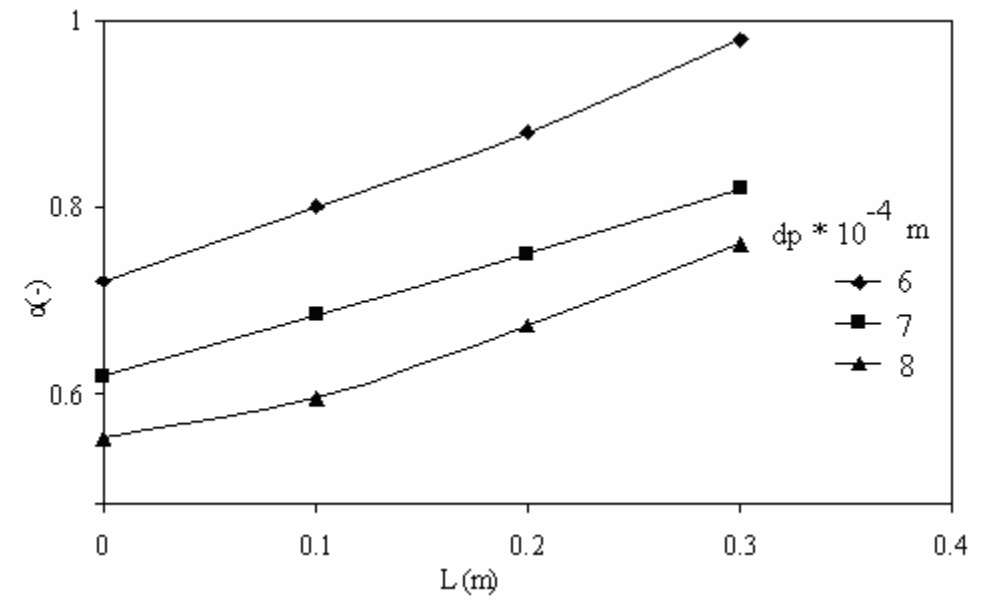

Figure 2: The effect of particle diameter on fraction of core layer, Q = $300x10^{-6}$ m^3 s^{-1}. ρ_s=8900 Kg m^{-3}.

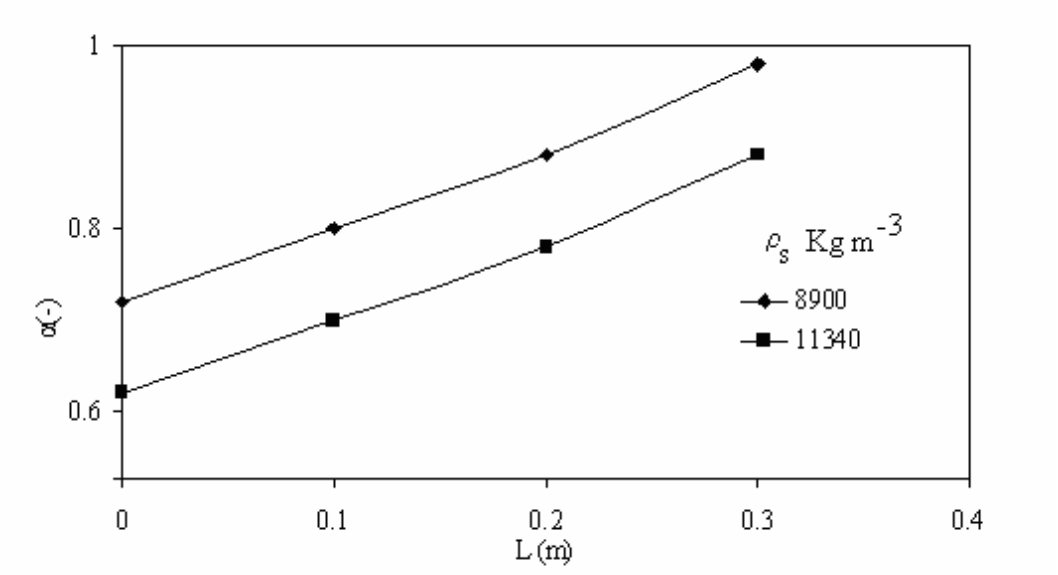

Figure 3: The effect of particle density on fraction of core layer, d_p= 0.06cm, Q= $300x10^{-6}$ m^3 s^{-1}.

The Figure 2 gives the variation of core layer thickness along the length of the fluidized bed electrode. It can be ascertained from the figure that the core layer thickness increases with increase in bed location along the riser. The core layer thickness is less at the bottom of the bed and increases with height. This can be explained that the electrolyte fed at the bottom of the bed accelerates the solids particles before attaining a steady state resulting less core layer thickness. It can also be ascertained from Figure 2 that the core layer thickness decreases with increase in the particle diameter. A decrease in core layer thickness with particle diameter is due to the fact that the particle terminal velocity increases with particle diameter and in turn the particle acceleration zone, which eventually decreases the core layer thickness.

Simulations have been carried out with two particle densities to verify the influence of particle density on the layer thickness. It can be ascertained from Figure 3 that an increase in the particle density decreases the core layer thickness. Increase in the particle density increases the terminal velocity of the particle and increases the acceleration zone resulting reduction in core layer thickness. On the other hand, the core layer thickness increases with increase in the electrolyte flowrate (Figure 4). This can be explained that an increase in the electrolyte flow rate increases the buoyancy offered by the fluid on the particles, which increases the particle flow resulting a reduction in the core layer thickness.

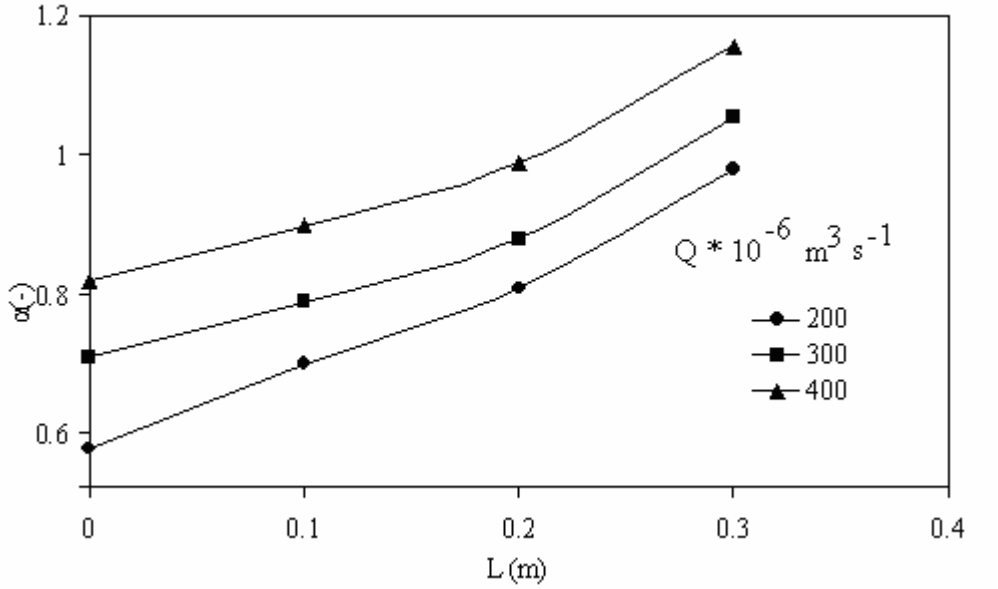

Figure 4: The effect of electrolyte flow rate on fraction of core layer, d_p= 0.06cm. ρ_s=8900 Kg m^{-3}.

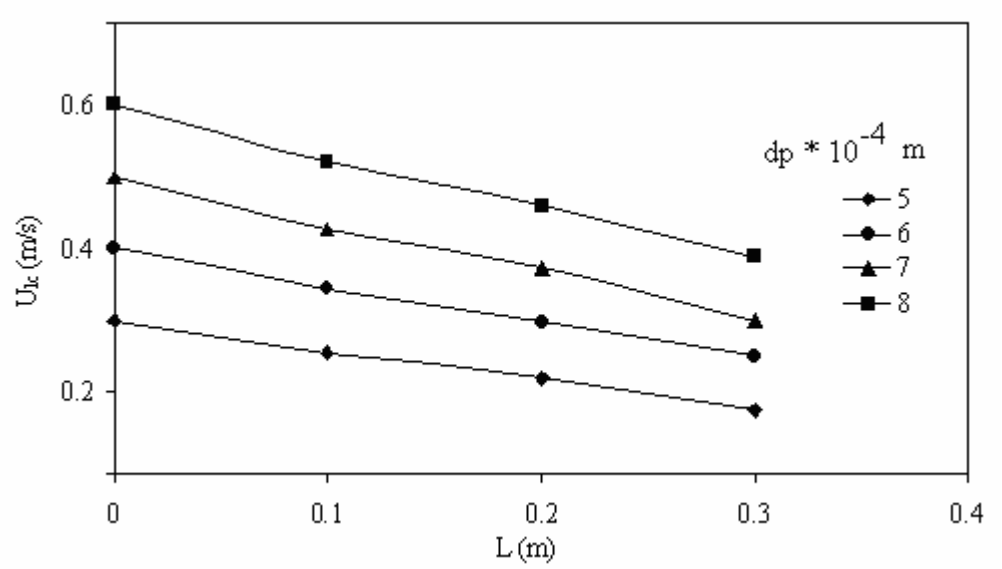

Figure 5: The effect of particle diameter on electrolyte velocity in core layer, Q=300x10^{-6} m^3 s^{-1}. ρ_s=8900 Kg m^{-3}.

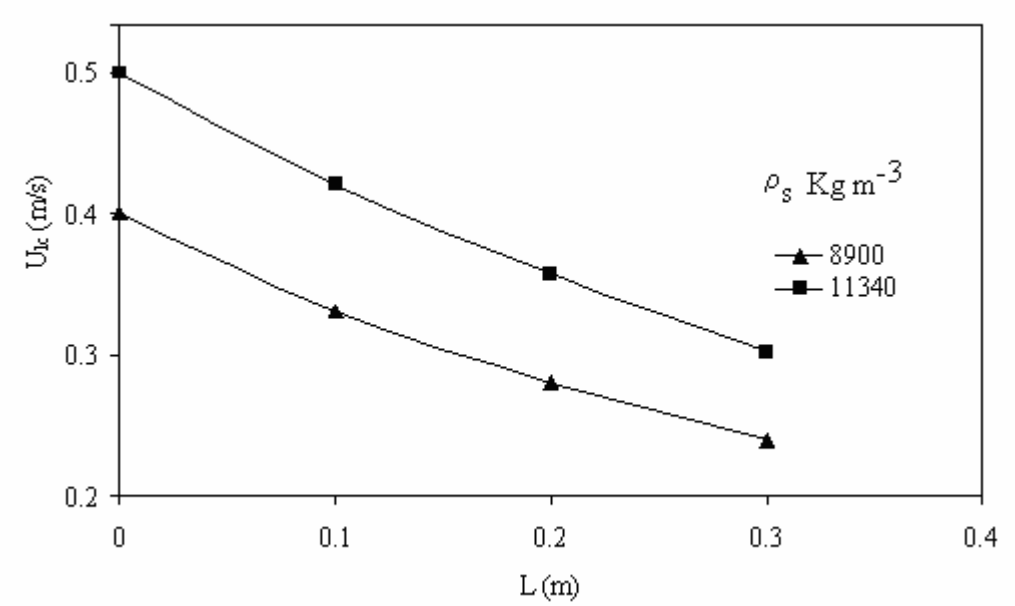

Figure 6: The effect of particle density on electrolyte velocity in the core layer, d_p=0.06 cm. Q= 300x10^{-6} m^3 s^{-1}.

Figures 5 & 6 show the effects of particle diameter and the particle density on the electrolyte velocity in the core layer (U_{lc}). It can be noticed from Figure 5 that the electrolyte velocity increased with increase in the particle diameter. For a given volumetric flow rate of the electrolyte, an increase in the particle diameter decreases the core layer thickness, i.e., the area available for electrolyte flow in the core layer, which eventually increases the electrolyte velocity in the core layer (Figure 5). Similarly the core layer thickness is decreased with increase in the particle size resulting increased electrolyte velocity in the core layer (Figure 6).

The effects of particle size, density and electrolyte flow rate on particle velocity in the core layer have been simulated and are given in Figures 7 to 9. The particle velocity decreases with bed depth (Figure 7). This can be explained that the core layer thickness increases with increase in the bed height for the given operating condition. Increase in the diameter of the core layer decreases the electrolyte velocity and in turn the particle velocity. The particle velocity increases with increase in the particle diameter. This is very interesting observation recorded in the present investigation. The particle velocity is expected to decrease with size for the given electrolyte velocity as the particle velocity directly proportional to its diameter. It has been observed earlier that the particle size reduces the thickness of the core layer (Figure 2) and the reduction in the core layer thickness increases the liquid rising velocity in the core layer. The increased electrolyte velocity in the core layer increases the particle velocity in spite of increased particle terminal velocity.

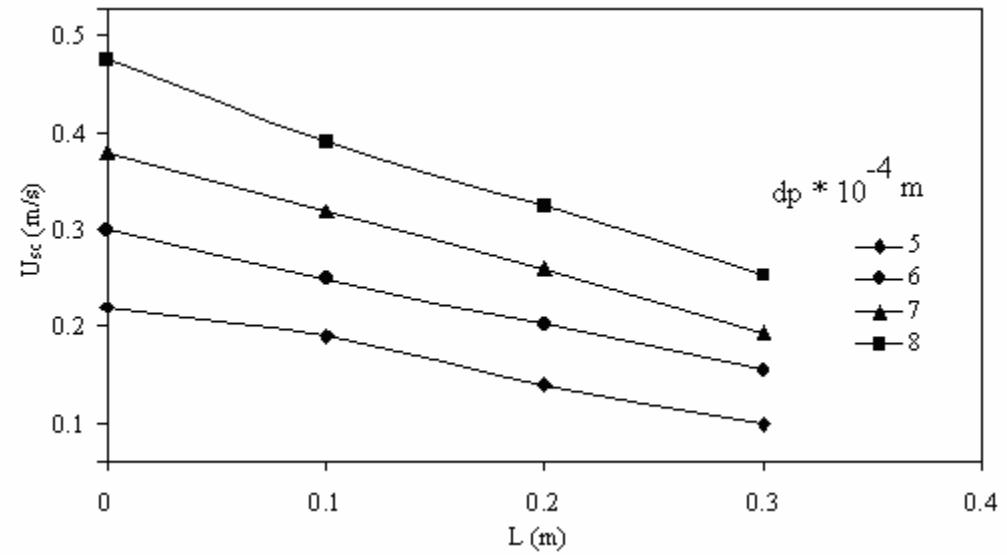

Figure 7: The effect of particle diameter on particle velocity in the core layer, $Q=300x10^{-6}$ m^3 s^{-1}. $\rho_s=8900$ Kg m^{-3}.

A similar observation has been recorded for the particle density on particle velocity in the core layer (Figure 8) as the particle density has same effect as particle diameter on the core layer thickness. An increase in the flow rate of the electrolyte for the given hydrodynamic condition, the electrolyte velocity in the core layer is increased and hence the particle velocity (Figure 9).

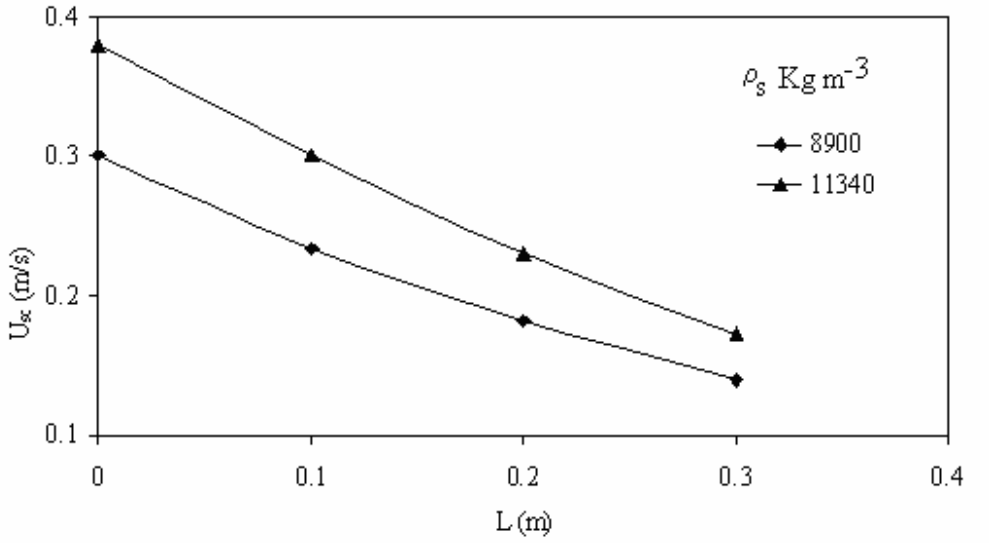

Figure 8: The effect of particle density on particle velocity in the core layer; d_p= 0.06cm; Q= 300x10^{-6} m^3 s^{-1}.

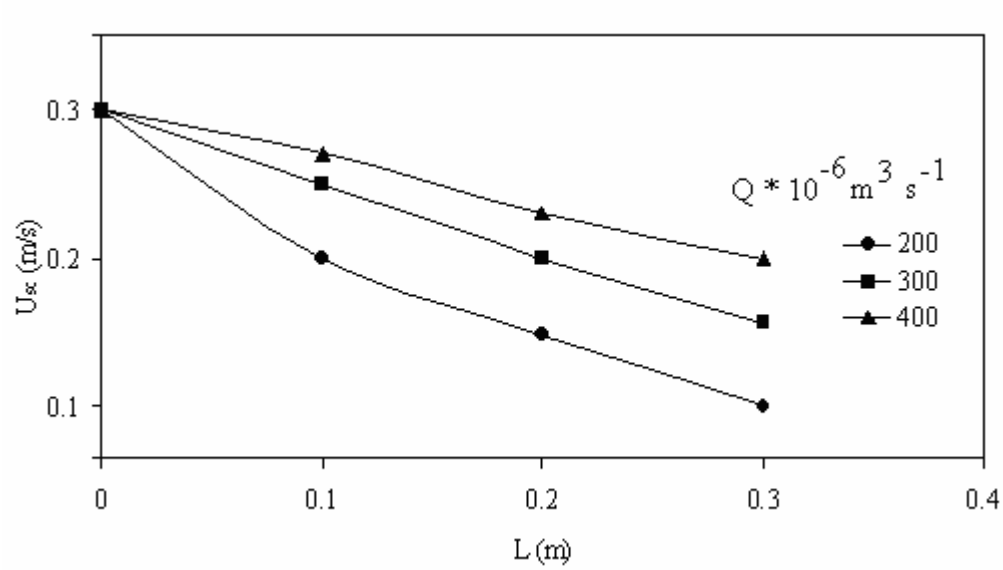

Figure 9: The effect of electrolyte flow rate on particle velocity in the core layer, d_p=0.06 cm. ρ_s=8900 Kg m^{-3}.

The electrolyte current density for a given operating condition is estimated using equation (33) and the simulated values are presented in Figure 10.

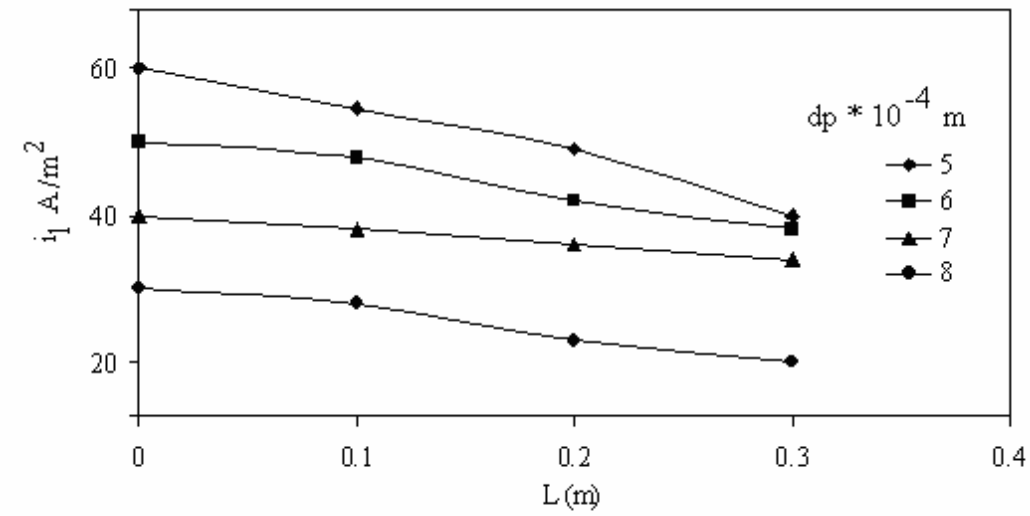

Figure 10: The effect of particle diameter on electrolyte current density distribution in the core layer, d_p= 0.06 cm, ρ_s=8900 Kg m^{-3}.

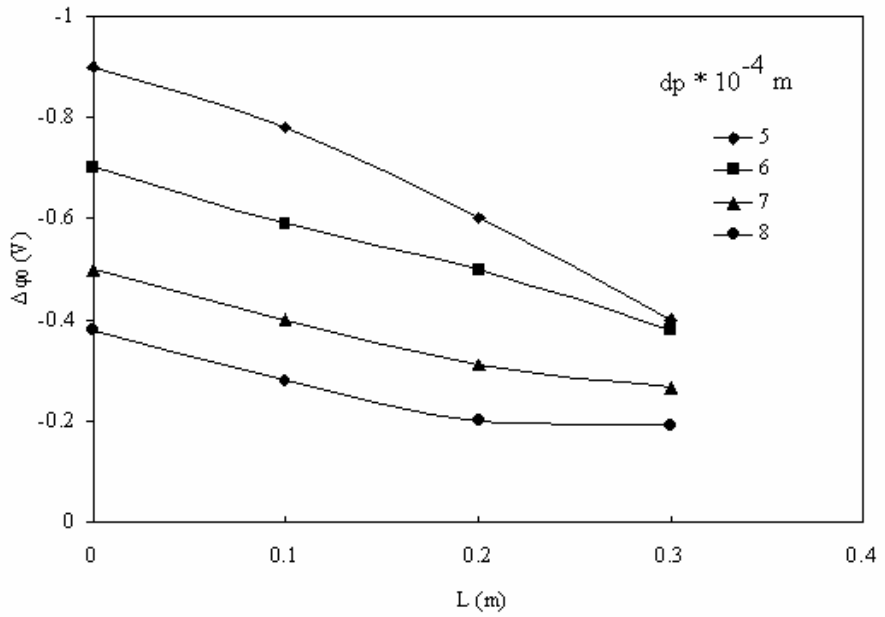

Figure 11: The effect of particle diameter on electrolyte potential distribution in the core layer, d_p= 0.06 cm, ρ_s=8900 Kg m^{-3}.

It can be ascertained from Figure 10 that the current density decreased with increase in the bed depth. While Figure 11 shows the simulated electrolyte potential along the reactor length for various particle sizes. It can be ascertained from the Figure 11 that the electrolyte potential decreases along the reactor length for a given operating condition. Further the electrolyte potential decreases with increases in the particle size. This may be due to the fact that the electrolyte potential is inversely proportional to the particle diameter (equation, 34).

The mass transfer coefficient has been simulated using equation (36) and the results are presented in Figure 12. It can be noticed from the Figure 12 that the mass transfer coefficient is increased with increase in the electrolyte velocity. It is obvious that the mass transfer coefficient is directly related to the electrolyte velocity and an increase in the particle size increases the electrolyte velocity and in turn the mass transfer coefficient.

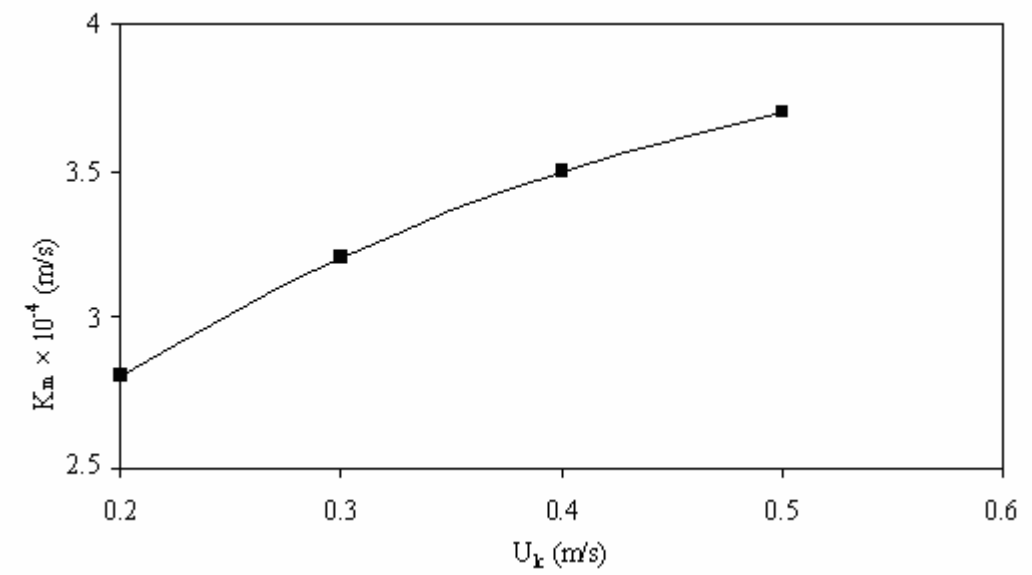

Figure 12: The effect of electrolyte velocity on mass transport coefficient in the core layer. ρ_s=8900 Kg m^{-3}, Q=300x10^{-6} m^3 s^{-1}.

It is attempted to validate the present model simulations with the data reported in the literature. The Figures 13 & 14 compares the present model simulation with the data reported due to Doherty et al (1995). It can be ascertained from the figures that the model simulation match satisfactorily with the experimental data reported in the literature.

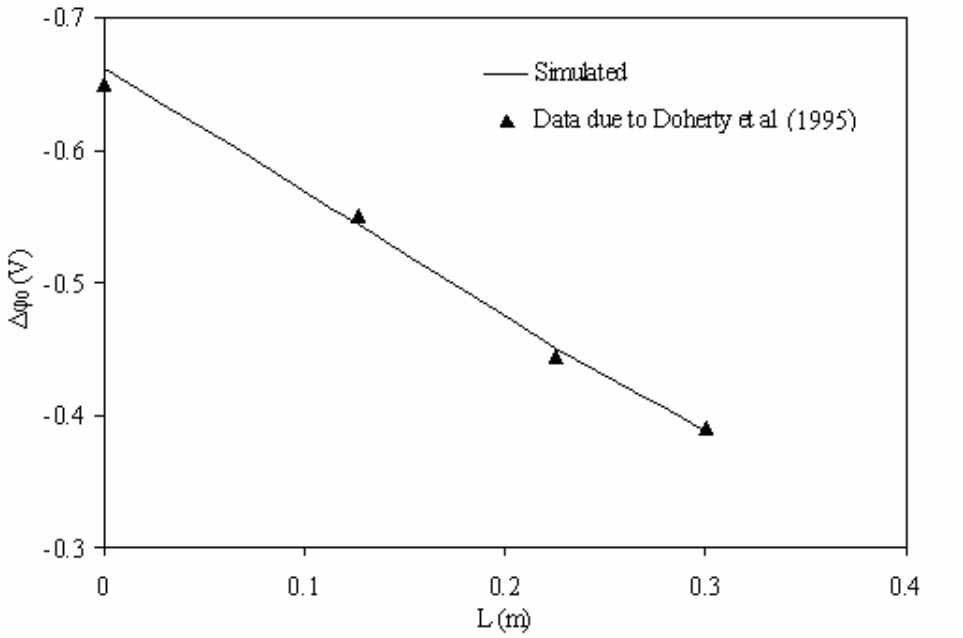

Figure 13: Comparison of the model prediction on decrease in electrolyte potential with the data reported due to Doherty et al. (1995).

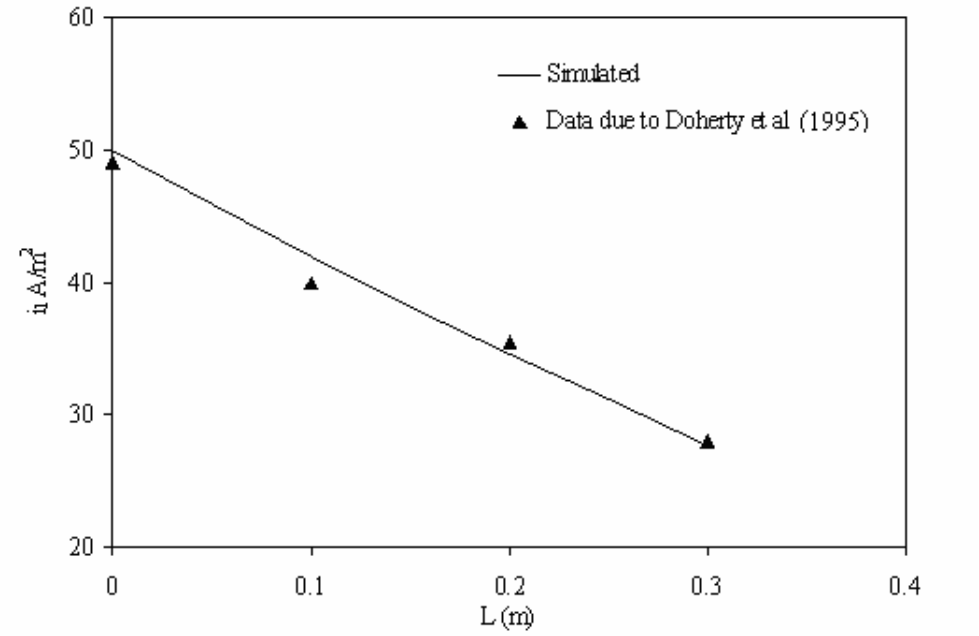

Figure 14: Comparison of model prediction on current density with the data reported due to Doherty et al (1995).

4. CONCLUSIONS

A core-annular flow model with transfer of particles between core-annular layers has been developed to describe the flow behavior of conducting particles and the electrolyte in the fluidized bed electrode. The effect of individual parameters on the rate of particle transfer across the layer and thickness of core-annular has been critically examined. The following conclusions are made:

1. The thickness of core layer increases with increase in the bed height and decrease with increase in particle diameter and density.
2. The thickness of the core layer increases with increase in the electrolyte flow rate.
3. The mass transfer coefficient depend the electrolyte velocity.

NOTATION

a	Specific surface area ($m^2\ m^{-3}$)
A	Cross sectional area of cell (m^2)
C_D	Drag Coefficient
Ci	Initial concentration of the effluent (M)
C_{out}	Final concentration of the effluent (M)
d	Pore diameter (m)
d_p	Particle diameter (10^2 m)
D	Diameter of the cell (m)
D_s	Diffusivity of solid particles ($m^2\ s^{-1}$)
F	Faraday constant (96,485 C)
g	Gravitational constant ($m\ s^{-2}$)
G_c	Solid mass flux ($Kg\ m^{-2}\ s^{-1}$)
i	Current density ($A\ m^{-2}$)
i_l	Electrolyte current density ($A\ m^{-2}$)
K	Solid transfer coefficient ($0.011\ m\ s^{-1}$)
K_m	Mass transport coefficient ($m\ s^{-1}$)
L_a	Height of particle inside the annular layer (m)
L_c	Height of particle inside the core layer (m)
L_o	Initial height of the bed (m)
M	Mass flow rate ($Kg\ s^{-1}$)
N	Number of electrons involved
n	Richardson and Zaki index
ΔP	Pressure drop ($Kg\ m^{-1}\ s^{-2}$)
Q	Electrolyte flow rate ($m^3\ s^{-1}$)
U_{la}	Electrolyte velocity in the annular layer ($m\ s^{-1}$)

U_{lc} Electrolyte velocity in the core layer (m s^{-1})
U_{mf} Minimum fluidization velocity (m s^{-1})
U_{sa} Particle velocity in the annular layer (m s^{-1})
U_{sc} Particle velocity in the core layer (m s^{-1})
U_{slip} Slip velocity (m s^{-1})
U_t Particle terminal velocity (m s^{-1})
V_c Current feeder potential (V)
Xi Conversion factor
ΔL Fractional height of the bed (m)
L Bed height (m)

Greek Letters

α^2 Fractional area occupied by the core layer
ε Bed voidage
ε_c Bed voidage in the core layer
ε_a Bed voidage in the annular layer
$\Delta\varphi_0$ Electrolyte potential (V)
κ_l Apparent electrolyte conductivity (S m^{-1})
κ_{lo} Electrolyte conductivity (S m^{-1})
μ_l Electrolyte Viscosity (Kg m^{-1} s^{-1})
ρ_S Solid particles density (Kg m^{-3})
ρ_l Electrolyte density (Kg m^{-3})

Subscripts

a Annular layer
c Core layer
l Electrolyte
mf minimum fluidization
p Solid particles

REFERENCES

Afsin, G., Nurdil, E., "Hydrodynamic modeling of a circulating fluidized bed", Powder Technology, Vol. 172, 1-13 (2007).

Backhurst, J.R, Good ridge, F., Coulson J.M, and Plimley R.E, "A preliminary investigation of fluidized bed electrodes", Journal of Electrochemical Society, Vol. 116, 1600-1607 (1969).

Couret, F., "The fluidized bed electrode for the continuous recovery of metals", Journal of Applied Electrochemistry, Vol. 10, 687-696 (1980).

Doherty, T., Sunderland, J.G., Roberts, E.P.L., Pickett, D.J., "An improved model of potential and current distribution within a flow-through porous

electrode", Electrochimica Acta, Vol. 41, 519-526 (1995).
Fleischmann, M., Oldfield, J. W., Tennakoon, L., "Fluidized bed electrodes part IV: Electro deposition of copper in a fluidized bed of copper-coated spheres", Journal of Applied Chemistry, Vol. 1, 103-112 (1971).
Good ridge, F., Scott K., "Electrochemical process engineering", Plenum Press New York, p 47 (1995).
Guohua Chen, "Electrochemical technologies on waste water treatment", Separation and purification technology, Vol. 38, 11-41 (2004).
Helland, E., Occelli, R., Tadrist, L., "Numerical study of cluster formation in a gas-particle circulating fluidized bed", Powder Technology Vol. 110**,** 210–221 (2000).
Kazdobin, K, Shvab, N. Tspakh S, "Scaling-up of fluidized-bed electrochemical reactors", Chemical engineering journal, Vol, 79, 203-209 (2000).
Kunii, D., Levenspiel, O., "Fluidization Engineering", Second Ed., Butterworth-Heinemann, Newton, MA, USA, (1991).
Lee, J.H., Ryu, G.H., "Electrochemical characteristics of graphite coated with tin-oxide and copper by fluidized-bed chemical vapour deposition", Journal of Power sources, Vol 107, 90-97 (2002).
LeRoy, L, "Fluidized bed electrowinning – I General modes of operation", Electrochimica acta, Vol. 23, 815-825 (1978).
LeRoy, L, "Fluidized bed electrowinning – II Operating at constant current density", Electrochimica acta, Vol. 23, 827-834 (1978).
Miura, H., Takahashi T., Ichikawa J., Kawase Y., "Bed expansion in liquid-solid two-phase fluidized beds with Newtonian and non-Newtonian fluids over the wide range of Reynolds numbers", Powder Technology, Vol. 117, 239-246 (2001).
Rhodes, M.J, "Modeling the Flow Structure of Upward-Flowing Gas-Solid suspensions", Powder Technology, Vol. 60**,** 27-38 (1990).
Savinell, R.F, Dweik B.M., "Hydrodynamic modeling of the liquid-solid behavior of the circulating particulate bed electrode", Journal of applied electrochemistry, Vol. 26**,** 1093 – 1102 (1996).
Scott, K., "Electrochemical reaction engineering", Academic Press (1991).
Welmers, A, Van Swaau, W. P. M., Beenackers, A. A. C. M., "Mechanism of charge transfer in the discontinuous metal phase of a fluidized bed electrode", Electrochimica acta, Vol. 22, 1277-1281 (1977).
Yerushalmi J., Cankurt N.T., Geldat D., Liss B., "Flow regimes in vertical gas-solid contacting systems". AIChE Symp. Ser. Vol. 74, 176, 1-6 (1978).
Zhoua, M., Wu, Z., Mab, X., Conga,Y., Yea, Q., Wang, D., "A novel fluidized electrochemical reactor for organic pollutant abatement", Separation and Purification Technology, 81-88 (2004).